

ISSN 1330–0008

CODEN FIZAE4

SURFACE SPECTRAL FUNCTIONS AND EXCITATION FREQUENCIES IN
THIN METALLIC FILMSVITO DESPOJA, LEONARDO MARUŠIĆ¹ and MARIJAN ŠUNJIĆ*Department of Physics, University of Zagreb, Bijenička 32, HR-10000 Zagreb, Croatia***Dedicated to the memory of Professor Vladimir Šips**

Received 25 October 2005; Accepted 28 November 2005

Online 7 December 2005

Surface spectral functions are calculated for very thin metal slabs, containing both collective modes and single-particle excitations. This is achieved by calculating the surface dielectric function $\varepsilon_p(\mathbf{Q}, \omega)$ for the thin jellium slab in the density functional theory and random phase approximation, using Kohn-Sham wavefunctions within the local density approximation, from which we derive the surface spectral functions. Influence of the slab thickness on the excitation spectra is studied, and the dispersion relations of the collective modes are obtained. Slightly modified fast converging method for the calculation of the Kohn-Sham wavefunctions is presented.

PACS numbers: 73.20.-r, 73.20.Mf, 73.21.-b

UDC 538.975

Keywords: surface spectral functions, collective modes, single-particle excitations, Kohn-Sham wavefunctions

1. Introduction

Study of electronic states and their excitations in thin metallic films, as described in a *jellium* model, is a standard problem in the physics of confined, quasi-two-dimensional systems. Its merit is partly practical, but mostly conceptual, and serves to clarify certain phenomena, either new or modified, in the systems with reduced symmetry. A variety of methods has been used and tested in this model, but local density approximation (LDA) in the Kohn-Sham (KS) scheme has proved to be most successful, in spite of its relatively demanding numerical requirements. While the ground-state properties have been studied extensively, and a number of useful results was obtained, numerical problems have prevented a complete systematic study of the electronic excitations for a wider range of parameters (film thickness and density), as well as their coupling to external probes.

Purpose of the study of the excitations in thin metallic slabs is usually to obtain the field produced by these excitations (outside or inside the solid) and to calcu-

¹Present address: Department of Transport and Maritime Studies, University of Zadar, M. Pavlinovića b.b., HR-23000 Zadar, Croatia

late the interaction of external particles (e.g. electrons or atoms) with that field. Results can then be related, e.g., to the LEED or EELS experiments, therefore this problem has been studied for a long time by a number of authors [1–13]. The study can be performed on various levels. One can, for example, take into account only collective (plasmon) modes, neglecting single-particle excitations, or perhaps study just the surface modes assuming that the bulk modes, due to screening, do not produce electric field outside the slab. That assumption is correct only in the long-wavelength limit; therefore, neglecting single-particle excitations makes sense only if we are interested in the field reasonably far away from the surface.

In systems like thin metallic films or metallic electrodes separated by a narrow gap (as in scanning tunneling microscope), electron is very close to the surface or even inside the solid, so we have to calculate the dynamical response by taking all single-particle and collective excitations into account, instead of limiting our calculations to collective modes dominant in the long-wavelength limit. We shall do this by relating the spectral function $S(\mathbf{Q}, \omega)$ to the polarizability $\tilde{\chi}_p(\mathbf{Q}, z, z', \omega)$ (p denoting parity), and calculating the polarizability within the random phase approximation (RPA) by use of the Kohn-Sham (KS) [1] wavefunctions in the local density approximation (LDA) [2].

A simple way to obtain the wavefunctions is the one based on the infinite barrier model (IBM) [3–5], where the wavefunctions are sinusoidal, therefore permitting an analytic calculation, leading to a very useful result. Although very valuable (primarily due to the remarkable simplicity), IBM fails to provide a quantitatively reliable result very close to the surface, and more sophisticated methods are needed. One possibility is to solve the KS equation for the jellium slab numerically, with the use of some corrections necessary to achieve the convergence of the iteration [2, 6], and another is to expand jellium wavefunctions in terms of sinusoidal IBM wavefunctions and solve a matrix version of the Kohn-Sham problem to obtain the expansion coefficients [7].

The wavefunctions could be also obtained for more realistic models of the crystal, including, e.g., surface periodic potential, using various *ab-initio* methods [8]. Then the system would not be translationally invariant but periodic (with reciprocal lattice vector \mathbf{G}) in the direction parallel to the surface. The response function would not be diagonal with respect to \mathbf{Q} , i.e. instead of $\chi_{qq'}(\mathbf{Q}, \omega)$, we would have $\chi_{qq'}(\mathbf{Q}, \mathbf{G}, \omega)$, which would complicate the calculation tremendously. Such calculations were done, e.g. to obtain a GW correction of the LDA exchange-correlation potential [9], or to calculate dynamical response and plasmon dispersion for the aluminum bulk [10], but only recently to determine surface plasmon dispersion and damping for a semi-infinite magnesium slab [14]. Therefore, we shall be using the jellium model which has the advantage of being translationally invariant in the direction parallel to the surface, but still allows relatively realistic description of charge fluctuations [15].

This approach can be applied to three different situations – a semi-infinite metal with only one surface, or a thin film or a metal-vacuum-metal system where we have two surfaces close to each other so that the modes on the surfaces are coupled (permitting one to study, e.g., electron tunneling in semiconductor heterostructures

or STM). In this paper, we shall study the thin film, but the other two cases can be derived from this one. In our previous work [11], we have already studied the excitation spectra in thin metallic slabs, but in this paper we concentrate on the influence of the slab thickness on the spectra and the dispersion relations.

We introduce a specific method for the solution of the KS equation based on the original Lang-Kohn method, and adjusted for the case of very thin slabs. Problem of the convergence of the iteration procedure limits the applicability of the method, and requires a careful choice of the initial electron density and iteration steps.

2. Formulation of the problem

The system we want to study is a thin metallic slab, with the thickness varying from several a_0 to several hundred a_0 . We shall use a jellium model, and assume our slab to be infinite in the $\rho = (x, y)$ plane, and finite in z direction, $-L < z < 0$. By that we mean that the electron density practically vanishes at the boundaries $z = -L$ and $z = 0$, with the positive background of thickness $d = L - 2a$, extending from $z = -L + a$ to $z = -a$ (Fig. 1). This means that the electron density decays outside the positive background, practically vanishing at some distance a .

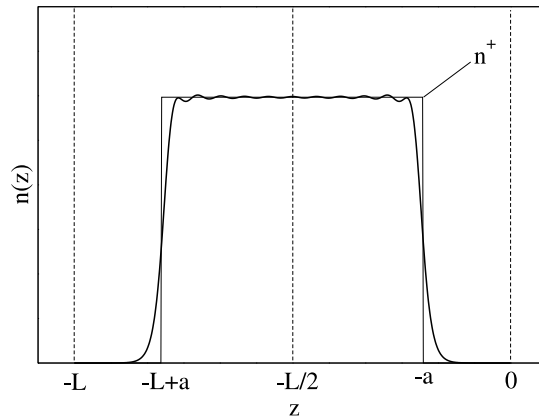


Fig. 1. Geometry of the slab, and the electron density profile. Positive background extends from $-L + a$ to $-a$. $n(z)$ is the electron charge density, and n^+ is the positive background charge density.

Therefore, all quantities can be Fourier transformed in the ρ direction as

$$f(\mathbf{Q}, z, z') = \int_{\tau} d\rho e^{i\mathbf{Q}\rho} f(\mathbf{r}, \mathbf{r}'), \quad (1)$$

$$f(\mathbf{r}, \mathbf{r}') = \frac{1}{(2\pi)^2} \int d\mathbf{Q} e^{-i\mathbf{Q}\rho} f(\mathbf{Q}, z, z'), \quad (2)$$

where τ is the total volume of the metal and \mathbf{Q} is the component of the wavevector parallel to the surface.

Wavefunctions can be written in the form

$$\Phi_{\nu}(\mathbf{r}) = \sqrt{\frac{2}{AL}} e^{i\mathbf{Q}\rho} \phi_j(z), \quad (3)$$

where $\nu = (\mathbf{Q}, j)$. Corresponding energies can be written as

$$E_\nu = \frac{\hbar^2 Q^2}{2m} + \epsilon_j, \quad (4)$$

where ϵ_j is the “perpendicular” part of the energy.

Since our slab is symmetrical with respect to the $z = -L/2$ plane, we can decompose charge fluctuation modes into symmetric ($p = +$) and antisymmetric ($p = -$) ones. Moreover, since in the linear response theory (anti)symmetric modes couple only with (anti)symmetric external perturbation, it is convenient to decompose our potentials into symmetric and antisymmetric parts, and treat them separately. That way our system will always have well defined symmetry, making it plausible to perform Fourier transform in the z direction by use of (anti)symmetrical functions

$$f_q^p = \int_{-L}^0 dz f(z) \cos qz, \quad f(z) = \frac{2}{L} \sum_q \eta_q f_q^p \cos qz, \quad (5)$$

where

$$q = \left\{ \begin{array}{ll} \frac{2n\pi}{L}, & p = + \\ \frac{(2n+1)\pi}{L}, & p = - \end{array} \right\}, \quad n = 0, 1, 2, \dots, \quad \eta_q = 1 - \frac{\delta_{q,0}}{2}. \quad (6)$$

Index p denotes that the q components of any quantity throughout this paper will have a well defined (even or odd) parity.

3. Excitation spectra

Spectral function of the surface modes can be written as [4, 11]

$$S_p(\mathbf{Q}, \omega) = \frac{1}{\pi} 2p e^{-QL} \text{Im} \frac{\epsilon_p(\mathbf{Q}, \omega)}{\epsilon_p(\mathbf{Q}, \omega) + 1}. \quad (7)$$

$\epsilon_p(\mathbf{Q}, \omega)$ is the surface dielectric function given by [3, 4, 11, 12]

$$\epsilon_p^{-1}(\mathbf{Q}, \omega) = \frac{4Q}{L} \sum_{qq'} \left[\frac{8\pi e^2}{L} \chi_{qq'}^p(\mathbf{Q}, \omega) + (Q^2 + q^2) \frac{\delta_{qq'}}{\eta_q} \right]^{-1}, \quad (8)$$

where $\chi_{qq'}^p$ are the Fourier components of the irreducible polarizability. In RPA, χ is replaced by the polarizability of the non-interacting electrons χ^0 , defined as

$$\chi^0(\mathbf{r}, \mathbf{r}', \omega) = \sum_{\nu, \nu'} \frac{f_\nu - f_{\nu'}}{E_\nu - E_{\nu'} - \hbar(\omega + i\eta)} \Phi_\nu(\mathbf{r}) \Phi_{\nu'}^*(\mathbf{r}) \Phi_{\nu'}(\mathbf{r}') \Phi_\nu^*(\mathbf{r}'), \quad (9)$$

with $f_\nu = 2\Theta(E_F - E_\nu)$, where E_F is the Fermi energy, $\Theta(x)$ is the Heaviside function and η is a positive infinitesimal. After Fourier transforming in the ρ direction,

and denoting the highest occupied state with j_M , one can write [13]

$$\chi^0(\mathbf{Q}, z, z', \omega) = \sum_{j=1}^{j_M} \sum_{j'=1}^{\infty} F_{jj'}(\mathbf{Q}, \omega) \phi_j(z) \phi_{j'}(z) \phi_j(z') \phi_{j'}(z'), \quad (10)$$

where $F_{jj'}(\mathbf{Q}, \omega)$ can be calculated analytically, and the result is

$$\begin{aligned} F_{jj'}(\mathbf{Q}, \omega) &= \frac{-1}{\pi Q^2} [2a_{jj'}(\mathbf{Q}) \\ &+ \operatorname{sgn}(\omega - a_{jj'}(\mathbf{Q})) \sqrt{(\omega - a_{jj'}(\mathbf{Q}) + i\eta)^2 - Q^2 k_j^2} \\ &- \operatorname{sgn}(\omega + a_{jj'}(\mathbf{Q})) \sqrt{(\omega + a_{jj'}(\mathbf{Q}) + i\eta)^2 - Q^2 k_j^2}], \end{aligned} \quad (11)$$

where

$$a_{jj'}(\mathbf{Q}) = \frac{\hbar}{2m} Q^2 - \frac{\epsilon_j - \epsilon_{j'}}{\hbar}, \quad k_j = \sqrt{\frac{2m}{\hbar} (E_F - \epsilon_j)}, \quad (12)$$

and ϵ_j is the “perpendicular” energy defined in (4).

Note that the Fourier transform, as defined in (5), necessary to obtain $\chi_{qq'}^{0p}$, can be calculated for z and z' separately, and we do it by means of a numerical integration. As always, it is done separately for even and odd parts, which means that the number of indices q is reduced by the factor two. Therefore, instead of having one matrix of order N containing even and odd contributions, we have two matrices each having order $N/2$ and containing only even or odd contributions. This significantly reduces the effort for matrix inversion in the calculation of the dielectric function from expression (8).

It might seem that infinite summation in (10) would cause a significant problem, but it turns out that the series converges reasonably fast, so we have to sum only the states up to three or four E_F , and these states are easily obtained.

If we use the free-electron wavefunctions in (9), then χ^0 reduces to the Lindhard response function of the free-electron gas. Much better approximation is obtained using the KS wavefunctions, i.e., the solutions of the z component of the Kohn-Sham equation, which can be obtained as described in the following section. In this way, we shall effectively go far beyond the standard RPA, except for vertex corrections of the irreducible polarizability.

4. Kohn-Sham wavefunctions

Kohn-Sham equation for the electronic wavefunctions is [1]

$$\left[-\frac{\hbar}{2m} \nabla^2 + V_{\text{eff}}(n, \mathbf{r}) \right] \Phi_i(\mathbf{r}) = E_i \Phi_i(\mathbf{r}), \quad (13)$$

with

$$V_{\text{eff}}(n, \mathbf{r}) = v(\mathbf{r}) + V_H(n, \mathbf{r}) + V_{xc}(n, \mathbf{r}), \quad (14)$$

where v is the external potential, V_H is the Hartree potential, V_{xc} is the exchange-correlation potential and n is the electron density.

Using the symmetry of our system, i.e. the Fourier transformations (1) and (2), and definitions (3) and (4), we can obtain a one-dimensional set of equations

$$\left[-\frac{\hbar^2}{2m} \frac{d^2}{dz^2} + V_{\text{eff}}(n, z) \right] \phi_l(z) = E_l \phi_l(z), \quad (15)$$

$$n(z) = \frac{1}{2\pi} \sum_j \phi_j^2(z) (E_F - E_j) \theta(E_F - E_j), \quad (16)$$

$$V_{\text{eff}}(z, n) = V_H(z, n) + V_{xc}^{\text{LDA}}(z, n), \quad (17)$$

where

$$V_H(z, n) = -2\pi \int [n(z') - n_+(z')] |z - z'| dz', \quad (18)$$

and the factor $(E_F - E_j)$ in (16) comes from the integration of the density of states.

Exchange-correlation potential V_{xc}^{LDA} can be calculated, e.g., from the Wigner expression [18] for exchange-correlation energy

$$\epsilon_{xc}(n(\mathbf{r})) = -\frac{0.458}{r_s(n(\mathbf{r}))} + \frac{0.44}{r_s(n(\mathbf{r})) + 7.8}. \quad (19)$$

Since the effective potential V_{eff} depends on the electron density, these equations have to be solved selfconsistently. In addition, the Fermi level for the metallic slab is not constant, as it is in the bulk or a semi-infinite metal, but varies with the slab thickness, i.e. with the number of the occupied energy levels, and it is defined by the expression for the positive background density

$$n_+ = \frac{1}{2\pi d} \sum_j \theta(E_F - E_j) (E_F - E_j). \quad (20)$$

It is well known that for a semi-infinite metal or a slab, selfconsistency can not be achieved by straightforward iteration. Namely, unlike the three-dimensional case, where the potential is proportional to $1/|\mathbf{r} - \mathbf{r}'|$, here, because of the one-dimensional transform $|z - z'|$, even a minute inaccuracy in the electron density at the point z' can have enormous influence on the potential at the point z if these points are far from each other. Therefore, several methods have been developed to obtain convergency [2, 6, 7]. In this paper we use a new method, similar to the previous ones, but modified to achieve the best results, i.e. fast convergence, for this particular problem.

5. Results and discussion

Using Eq. (7), we calculated spectral functions of even and odd surface excitations in a metallic (jellium) slab with the density $r_s = 2$, similar to aluminium,

and for three different slab thicknesses, $d = 10 a_0$, $50 a_0$ and $100 a_0$. The results are shown in Fig. 2. For a thin slab (Fig. 2a) and for $Q = 0.05 k_F$, the even (symmetric) collective mode is easily distinguished from the single-particle continuum, while the odd (antisymmetric) mode is much less pronounced, and it is almost impossible to

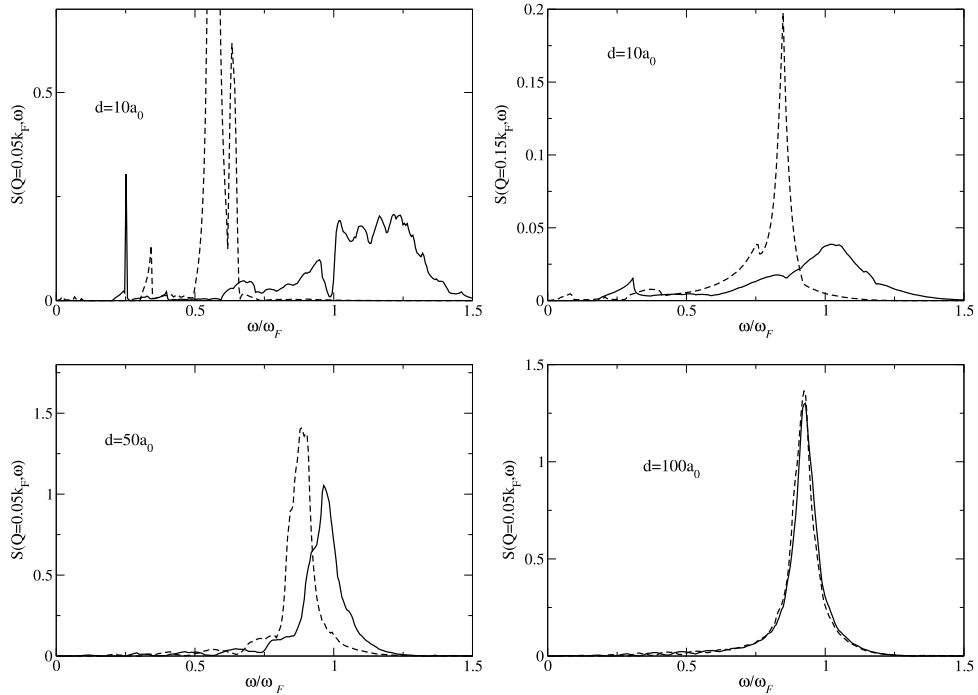


Fig. 2. Spectral function $S(\mathbf{Q}, \omega)$ of surface excitations for three different slab thicknesses d (as indicated on the figure), and for fixed values of Q . Full line is for odd modes, and dashed line for even modes.

identify it among the electron-hole excitations. The reason is that in such a thin slab at small wavevectors (i.e. large wavelengths), the even mode behaves almost like a (quasi) two-dimensional plasmon with dispersion $\omega_- \propto \sqrt{Q}$, while the odd mode cannot be formed properly. For $Q = 0.15 k_F$ (Fig. 2b), this is still visible, i.e. the even mode gives a sharp peak, while the odd mode is less pronounced, and we also observe single-particle contributions at smaller energies. For $d = 50 a_0$ (Fig. 2c), both peaks are well defined, but single-particle spectrum is suppressed at small wavevectors. For even larger thickness, $d = 100 a_0$ (Fig. 2d), both peaks occur at the same frequency already for $Q = 0.05 k_F$.

Figure 3 shows the dispersion relations obtained by following the peaks in the spectral functions calculated for three thicknesses and different wavevectors. They show the expected qualitative behavior, but it can be seen that quantitatively they differ from the classical result

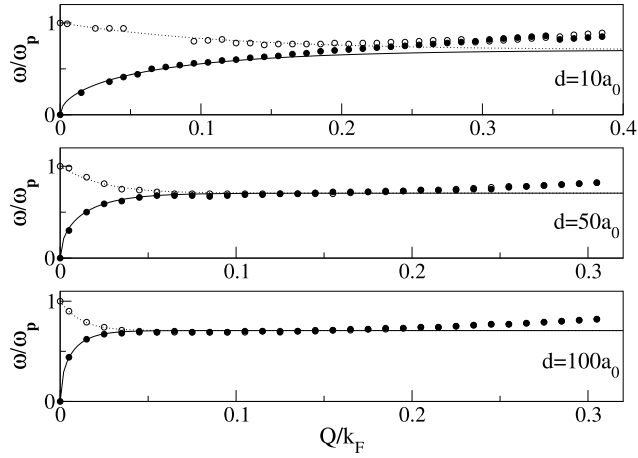


Fig. 3. Dispersion relations of surface collective modes obtained from the peaks in the spectral functions (dots), compared to the classical result (lines). Full lines and full dots are for odd modes, while dashed lines and circles for even modes.

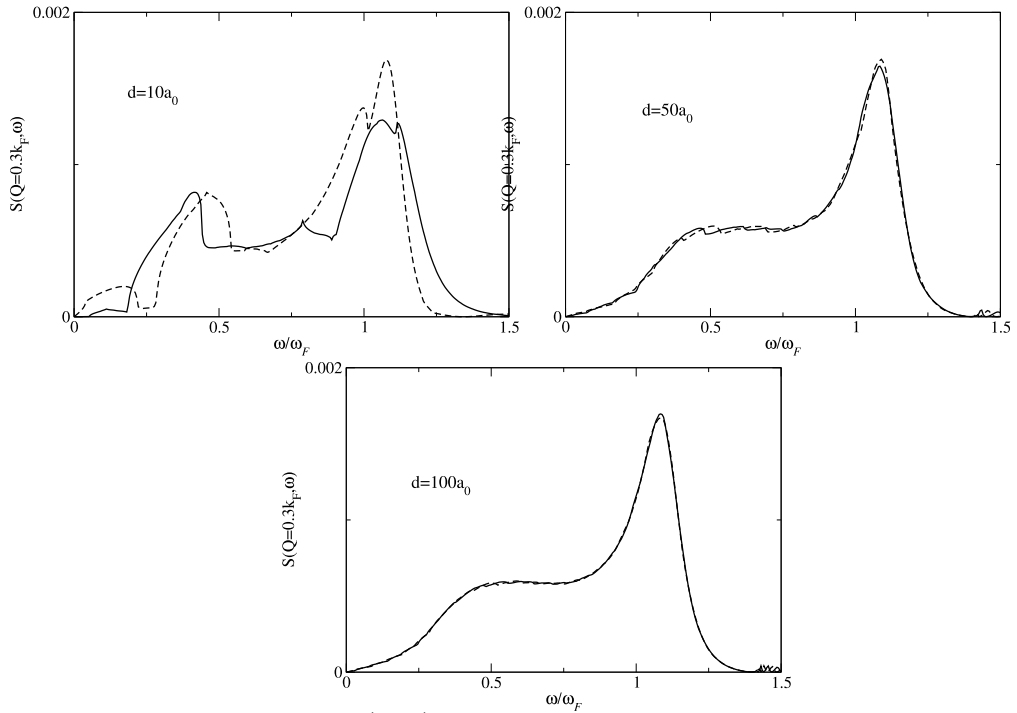


Fig. 4. Spectral function $S(\mathbf{Q}, \omega)$ for three slab thicknesses d and for $Q = 0.3K_F$, illustrating gradual suppression of the collective modes by single-particle excitations. Full line is for odd modes, and dashed line for even modes.

$$\omega_{\pm} = \frac{\omega_p}{\sqrt{2}} (1 \pm e^{-Qd})^{1/2}, \quad (21)$$

also shown in Fig. 3. It is significant that for large Q , the frequencies of both surface plasmons do not converge to ω_s , but continue increasing, though it becomes difficult to distinguish them from the single-particle continuum, as shown in Fig. 4 for $Q = 0.3 k_F$. Such result is in agreement with the well known dispersion of the bulk plasmons as well as with the experimental results for the semi-infinite metals [19]. For a very thin slab ($d = 10 a_0$), we could identify very few points corresponding to odd modes at small wave-vectors, because, as explained earlier, it is difficult to distinguish these modes from the single-particle excitations.

Figure 4 shows spectra for larger wave-vectors ($Q = 0.3 k_F$) for the same three slab thicknesses. Clearly, in all three cases the electron-hole continuum becomes more significant, taking away the intensity from the collective modes, and the difference between even and odd modes gradually disappears (especially for thicker slabs). For even larger wavevectors, collective modes become completely suppressed by the single-particle continuum.

6. Conclusion

Main objective of this paper was to perform a complete study of the excitation spectra in metallic slabs thick approximately from $10 a_0$ to $100 a_0$, and analyze how the slab thickness influences the spectra. To achieve that, we had to develop not only the method for the calculation of the spectra (described in Section 3), but also the method for the calculation of the KS wavefunctions necessary to include the proper response which contains collective modes and single-particle excitations (Section 4). In order to achieve the convergency of the Kohn-Sham scheme, we developed a computational method described in more detail in the Appendix. In that way we were able to calculate the excitation spectra and dispersion relations, described and discussed in Section 5.

Appendix

Selfconsistent solution of Eqs. (15), (16) and (17) is, in principle, obtained by the iteration procedure. We can start from some model-potential V_{eff}^0 , solve Eq. (15), use the obtained wavefunctions to calculate the density and first-iteration effective potential V_{eff}^1 , etc. until we reach selfconsistency; or we can assume some model-density n^0 and start the iteration from that point. In either case, as it is well known, it turns out that selfconsistency cannot be reached by straightforward iterations, and at each step some additional corrections are needed.

This problem was first solved by Lang and Kohn [2] in 1970 for a semi-infinite metal, and by Schulte [6] for a metallic slab. Lang and Kohn started from the model-density, while Schulte started from the model-potential, and the corrections they performed were designed for the particular problem they were solving and the

procedure they were using. The same problem was also solved by Eguiluz et al. [7] who expanded the wavefunctions in terms of plane waves. In the latter approach, they were able to achieve selfconsistency by iteration without additional corrections, but they needed several hundred iterations, while the previously mentioned methods required only a few iterations.

We use the combination of the first two methods. We start from the model-density, like Lang and Kohn, because, in our opinion, it is easier to construct an appropriate density than the potential. However, the rest of our calculation scheme is more similar to that developed by Schulte because we are dealing with the same system, i.e. a thin metallic slab.

If the iteration procedure starts from the density, then the density n_i is used to construct the effective potential for which we calculate the wavefunctions, and use them to obtain the density n_{i+1} . This procedure can be formally written as a functional, i.e.

$$n_{i+1}(z) = F[n_i, z], \quad (22)$$

and the selfconsistency problem can be reduced to the calculation of the correction δn which satisfies the following condition

$$n(z) + \delta n(z) = F[n + \delta n, z]. \quad (23)$$

We start from the model-density n_0 having a remarkably simple form

$$n_0(z) = n_+ \begin{cases} A e^{\alpha(z+L-a)}, & z < -L + a \\ 1 - B e^{-\beta(z+L-a)}, & -L + a \leq z \leq -\frac{L}{2} \\ 1 - B e^{\beta(z+a)}, & -\frac{L}{2} < z \leq -a \\ A e^{-\alpha(z-a)}, & z > -a, \end{cases} \quad (24)$$

where n_+ is the positive background density given by Eq. (20), which we use to determine the appropriate Fermi level. There are four parameters, A , B , α and β , two of which can be determined from the condition that the density and its first derivative must be continuous at the point $z = d/2$, while the other two can be varied to obtain the model-density most suitable for further iterations. It could seem that one more parameter should be determined from the requirement that the system should satisfy charge neutrality, but it turns out that even if the model-density does not meet that requirement, the calculated density does because it is automatically taken care of through the calculation of the Fermi level.

It could also seem that Eq. (24) is a poor choice for the model-density, i.e. that such choice is one of the reasons why the straightforward iteration procedure is not convergent, and that inside the jellium we should use a function that simulates Friedel oscillations. However, that is not the case because the major influence on the potential at some point inside the jellium comes from the density far away from it, so it is much more important to have a good approximation in that area. In fact, because of the form of the one-dimensional Hartree potential, even if we take a selfconsistent solution, obtained through our procedure as a starting point, the straightforward iteration will still diverge.

We start our procedure by varying the parameters to obtain the best possible model-density (24), the one for which the difference between the first and second iteration density is minimal. We achieve that by varying parameters until the integral

$$\int_{-\infty}^{\infty} \left(\frac{n_1(z) - n_2(z)}{n_+} \right)^2 dz$$

is sufficiently small. Since the density satisfies $n_2(z) = F[n_1, z]$, after expanding the functional F up to the first order, the self-consistency condition (23) can be rewritten as

$$\delta n(z) = n_2(z) - n_1(z) + \int G(z, z') \delta n(z') dz', \quad (25)$$

where

$$G(z, z') = \frac{F[n_1, z]}{\delta n_1(z')}. \quad (26)$$

Just like the initial set of Eqs. (15) – (20), the integral Eq. (25) cannot be solved selfconsistently by iteration, so it is better to rewrite it in the matrix form and solve the resulting set of algebraic equations.

Instead of continuous variables z and z' , we use discrete points z_i and z_j respectively, leading to the matrix equation

$$\sum_j [G_{ij} - \delta_{ij}] \delta n_j = \Delta n_i, \quad (27)$$

where $\Delta n_i = n_1(z_i) - n_2(z_i)$, and the matrix elements G_{ij} are

$$G_{ij} = \frac{\delta F[\{n_1(z_k)\}, z_i]}{\delta n(z_j)} = \frac{F[n_1(z_j), z_i] - F[n_1(z_j) - \lambda n_1(z_j), z_i]}{\lambda n_1(z_j)}, \quad (28)$$

where λ is an arbitrarily small number. In other words, G_{ij} represents the response of the functional F at the point z_i to the small variation of the density at the point z_j .

Solving Eq. (25) does not result in the self consistent solution of the initial problem, but gives us a better value for n_1 , from which we can calculate a new n_2 , and solve Eq. (25) again. After repeating such a procedure several times (usually five) we reach a satisfactory solution.

References

- [1] P. Hohenberg and W. Kohn, Phys. Rev. **136** (1964) B864; W. Kohn and L. J. Sham, Phys. Rev. **140** (1965) A1133.
- [2] N. D. Lang and W. Kohn, Phys. Rev. B **1** (1970) 4555.
- [3] D. M. Newns, Phys. Rev. B **1** (1970) 3304.
- [4] Z. Penzar and M. Šunjić, Phys. Scr. **30** (1984) 431, and Solid State Commun. **46** (1983) 385.

- [5] D. E. Beck and V. Celli, Phys. Rev. B **2** (1970) 2955; A. Griffin and E. Zaremba, Phys. Rev. A **8** (1973) 486; P. Hertel, Surf. Sci. **69** (1977) 237; E. Wikborg and J. E. Ingelsfeld, Phys. Scr. **15** (1977) 37; G. Korzeniewski, T. Maniv and H. Metiu, J. Chem. Phys. **76** (1982) 1564.
- [6] F. K. Schulte, Surf. Sci. **55** (1976) 427.
- [7] A. G. Eguiluz, D. A. Campbell, A. A. Maradudin and R. F. Wallis, Phys. Rev. B **30** (1984) 5449.
- [8] A review of this research can be found, e.g., in M. C. Payne, M. P. Teter, D. C. Allan, T. A. Arias and J. D. Joannopoulos, Rev. Mod. Phys. **64** (1992) 1045.
- [9] A. G. Eguiluz, M. Heinrichsmeier, A. Fleszar and W. Hanke, Phys. Rev. Lett. **68** (1992) 1359.
- [10] A. A. Quong and A. G. Eguiluz, Phys. Rev. Lett. **70** (1993) 3955.
- [11] L. Marušić and M. Šunjić, Phys. Scr. **63** (2001) 336.
- [12] L. Marušić and M. Šunjić, Fizika A (Zagreb) **7** (1998) 145.
- [13] A. G. Eguiluz, Phys. Rev. B **31** (1985) 3303.
- [14] V. M. Silkin, E. V. Chulkov and P. M. Echenique, Phys. Rev. Lett. **93** (2004) 176801.
- [15] One could also mention similar though less complete calculation by W. L. Schaich and J. F. Dobson Phys. Rev. B **49** (1994) 14700, and a number of theoretical calculations of surface plasmons in semi-infinite systems, mostly concerned with their low Q limit [16], or the discussion of ‘multipole plasmons’ (e.g. [17]).
- [16] E.g., P. J. Feibelman and K. D. Tsuei, Phys. Rev. B **41** (1990) 8519; W. L. Schaich, Phys. Rev. B **55** (1996) 9379; A. Liebsch, Phys. Rev. Lett. **71** (1993) 145.
- [17] J. Sellares and N. Barberan, Phys. Rev. B **50** (1994) 1879.
- [18] E. P. Wigner, Phys. Rev. **40** (1934) 1002.
- [19] E.g., K.-D. Tsuei, E. W. Plummer and P. J. Feibelman, Phys. Rev. Lett. **63** (1989) 2256; S. Suto, K.-D. Tsuei, E. W. Plummer and E. Burstein, Phys. Rev. Lett. **63** (1989) 2590; G. Chiarello, et al., Phys. Rev. B **62** (2000) 12676.

POVRŠINSKE SPEKTRALNE FUNKCIJE I FREKVENCIJE POBUĐENJA U TANKIM METALNIM SLOJEVIMA

Izračunali smo površinske spektralne funkcije vrlo tankih metalnih slojeva koje sadrže kolektivne modove i jednočestična pobuđenja. To smo postigli računanjem površinske dielektrične funkcije $\epsilon_p(\mathbf{Q}, \omega)$ za tanak sloj elektronskog plina u teoriji funkcionala gustoće i aproksimaciji slučajnih faza, primjenom Kohn-Shamovih valnih funkcija u aproksimaciji lokalne gustoće, na osnovi koje se izvode površinske spektralne funkcije. Proučavali smo utjecaj debljine sloja na spektre pobuđenja i dobili disperzijske relacije za kolektivne modove. Izložimo malo promijenjenu metodu za računanje Kohn-Shamovih valnih funkcija koja brzo konvergira.